Synthesis and preliminary biological evaluation of O-2((2-[(18)F]fluoroethyl)methylamino)ethyltyrosine ([(18)F]FEMAET) as a potential cationic amino acid PET tracer for tumor imaging

Chiotellis, Aristeidis ; Müller, Adrienne ; Weyermann, Karin ; Leutwiler, Dominique S ; Schibli, Roger ; Ametamey, Simon M ; Krämer, Stefanie D ; Mu, Linjing

Abstract: Amino acid transport is an attractive target for oncologic imaging. Despite a high demand of cancer cells for cationic amino acids, their potential as PET probes remains unexplored. Arginine, in particular, is involved in a number of biosynthetic pathways that significantly influence carcinogenesis and tumor biology. Cationic amino acids are transported by several cationic transport systems including, ATB(0,+) (SLC6A14), which is upregulated in certain human cancers including cervical, colorectal and estrogen receptor-positive breast cancer. In this work, we report the synthesis and preliminary biological evaluation of a new cationic analog of the clinically used PET tumor imaging agent O-(2-[(18)F]fluroethyl)-L-tyrosine ([(18)F]FET), namely O-2((2-[(18)F]fluoroethyl)methylamino)ethyltyrosine ([(18)F]FEMAET). Reference compound and precursor were prepared by multi-step approaches. Radiosynthesis was achieved by no-carrier-added nucleophilic [(18)F]fluorination in 16-20% decay-corrected yields with radiochemical purity >99%. The new tracer showed good stability in vitro and in vivo. Cell uptake assays demonstrated that FEMAET and [(18)F]FEMAET accumulate in prostate cancer (PC-3) and small cell lung cancer cells (NCI-H69), with an energy-dependent mechanism. Small animal PET imaging with NCI-H69 xenograft-bearing mice revealed good tumor visualization comparable to [(18)F]FET and low brain uptake, indicating negligible transport across the blood-brain barrier. In conclusion, the non-natural cationic amino acid PET probe [(18)F]FEMAET accumulates in cancer cells in vitro and in vivo with possible involvement of ATB(0,+).

DOI: https://doi.org/10.1007/s00726-014-1754-7

Amino Acids (2014) 46:1947–1959
DOI 10.1007/s00726-014-1754-7

ORIGINAL ARTICLE

Synthesis and preliminary biological evaluation of *O*-2((2-[^{18}F]fluoroethyl)methylamino)ethyltyrosine ([^{18}F]FEMAET) as a potential cationic amino acid PET tracer for tumor imaging

Aristeidis Chiotellis · Adrienne Müller · Karin Weyermann · Dominique S. Leutwiler · Roger Schibli · Simon M. Ametamey · Stefanie D. Krämer · Linjing Mu

Received: 5 July 2013 / Accepted: 19 April 2014 / Published online: 7 May 2014

Abstract Amino acid transport is an attractive target for oncologic imaging. Despite a high demand of cancer cells for cationic amino acids, their potential as PET probes remains unexplored. Arginine, in particular, is involved in a number of biosynthetic pathways that significantly influence carcinogenesis and tumor biology. Cationic amino acids are transported by several cationic transport systems including, $ATB^{0,+}$ (SLC6A14), which is upregulated in certain human cancers including cervical, colorectal and estrogen receptor-positive breast cancer. In this work, we report the synthesis and preliminary biological evaluation of a new cationic analog of the clinically used PET tumor imaging agent *O*-(2-[^{18}F]fluoroethyl)-L-tyrosine ([^{18}F]FET), namely *O*-2((2-[^{18}F]fluoroethyl)methylamino)ethyltyrosine ([^{18}F]FEMAET). Reference compound and precursor were prepared by multi-step approaches. Radiosynthesis was achieved by no-carrier-added nucleophilic [^{18}F]fluorination in 16–20 % decay-corrected yields with radiochemical purity >99 %. The new tracer showed good stability in vitro and in vivo. Cell uptake assays demonstrated that FEMAET and [^{18}F]FEMAET accumulate in prostate cancer (PC-3) and small cell lung cancer cells (NCI-H69), with an energy-dependent mechanism. Small animal PET imaging with NCI-H69 xenograft-bearing mice revealed good tumor visualization comparable to [^{18}F]FET and low brain uptake, indicating negligible transport across the blood–brain barrier. In conclusion, the non-natural cationic amino acid PET probe [^{18}F]FEMAET accumulates in cancer cells in vitro and in vivo with possible involvement of $ATB^{0,+}$.

Keywords Cationic amino acids · PET · Tumor imaging · Amino acid transporter · ATB^{0+} · SLC6A14

Abbreviations

[^{18}F]FDG	2-[^{18}F]fluoro-2-deoxy-D-glucose
mTOR	Mammalian target of rapamycin
LAT1	System L amino acid transporter
[^{18}F]FET	*O*-(2-[^{18}F]fluroethyl)-L-tyrosine
CAT	Cationic amino acid transporter family
NO	Nitric oxide
[^{18}F]AFETP	(*S*)-2-amino-3-[1-(2-[^{18}F]fluoroethyl)-1*H*-[1,2,3]triazol-4-yl]propanoic acid
[^{18}F]FEMAET	*O*-2((2-[^{18}F]fluoroethyl)methylamino) ethyltyrosine
DEAD	Diethyl azodicarboxylate
KCN	Potassium cyanide
DIPEA	Diisopropylethylamine
DAST	Diethylaminosulfurtrifluoride
CBr_4	Carbon tetrabromide
PPh_3	Triphenylphosphine
[^{18}F]FDOPA	L-3,4-Dihydroxy-6-[^{18}F]fluorophenylalanine
EBSS	EARLE balanced salt solution

Introduction

Non-invasive imaging is an essential component of the diagnosis, staging and therapeutic monitoring of cancer.

A. Chiotellis · A. Müller · K. Weyermann · D. S. Leutwiler · R. Schibli · S. M. Ametamey · S. D. Krämer
Center for Radiopharmaceutical Sciences ETH-PSI-USZ, Institute of Pharmaceutical Sciences ETH, Zurich, Switzerland

D. S. Leutwiler · L. Mu (✉)
Department of Nuclear Medicine, Center for Radiopharmaceutical Sciences ETH-PSI-USZ, University Hospital, Zurich, Switzerland
e-mail: linjing.mu@usz.ch

Among the various imaging modalities, PET is a radiotracer-based imaging method that has been recognized as a powerful tool, able to provide molecular and physiological information for diverse cancer lesions (McConathy and Goodman 2008; McConathy et al. 2012). Since a common feature of cancer cells is a high demand for nutrients (e.g., glucose, amino acids, fatty acids, vitamins and micronutrients) to support their fast growth and proliferation, there is a strong rationale for using such compounds as PET probes (Ganapathy et al. 2009; Plathow and Weber 2008).

Radiolabeled amino acids are a promising class of tracers for imaging upregulated metabolism associated with several hallmarks of cancer. These tracers have the potential to overcome some of the limitations of 2-[^{18}F]fluoro-2-deoxy-D-glucose ([^{18}F]FDG), the most commonly used oncologic PET tracer, mainly because of their low uptake in healthy brain and inflammatory tissue (Kaim et al. 2002; Lee et al. 2009; Shreve et al. 1999). Moreover, some of them may be useful for slowly growing tumors such as renal cell carcinoma and endocrine tumors where [^{18}F]FDG shows low or variable uptake (Koopmans et al. 2009; Schoder and Larson 2004; Sundin et al. 2004, 2007). There is also increasing evidence that the enhanced uptake of amino acids is correlated with signaling pathways involved in tumor growth, including the mammalian target of rapamycin (mTOR) pathway (Beugnet et al. 2003) and may have prognostic significance.

Amino acids generally enter cells through membrane-associated carrier proteins, and more than 20 distinct amino acid transporters have been identified in mammalian cells differing in terms of substrate specificity, tissue expression patterns, dependence on sodium and other ions, sensitivity to pH and mechanism of transport (McConathy et al. 2012). Tumor cells have a distinct metabolic need for amino acids to support their rapid growth, serving different needs such as protein synthesis, energy production, cell signaling and as a carbon and nitrogen source for cell growth (Ganapathy et al. 2009). This high demand is met by an enhanced cellular entry of amino acids through upregulation of certain of the aforementioned transporters (Busch et al. 1959; Fuchs and Bode 2005; Saier et al. 1988). Among these, the L-type amino acid transporter 1 (LAT1), an obligatory exchange, sodium-independent neutral amino acid transporter, has been the center of attention because of its critical role in angiogenesis, tumor growth and proliferation (Kim et al. 2004; Kobayashi et al. 2008; Nawashiro et al. 2006; Tamai et al. 2001; Fuchs and Bode 2005). A number of labeled amino acids targeting system L have demonstrated promising clinical utility with *O*-(2-[^{18}F]fluroethyl)-L-tyrosine ([^{18}F]FET) (Langen et al. 2006; Wester et al. 1999) being one of the most successful examples (Fig. 1).

Recently, there has been growing interest in other amino acid transport systems which are implicated in cancer growth, including xCT, (Ganapathy et al. 2009; Nakanishi and Tamai 2011) glutamine (Wise and Thompson 2010) and cationic amino acid transporters. The entry of basic amino acids (L-lysine, L-histidine and L-arginine) into cells can be mediated by several sodium-independent or sodium-dependent transporter systems, including the cationic amino acid transporter (CAT) family, system y^+L, $b^{0,+}AT$, and $ATB^{0,+}$ (Closs 2002; Closs et al. 2006; Kanai et al. 2000). Both L-lysine and L-histidine are essential amino acids that cannot be synthesized by human cells. L-arginine, although conditionally essential, is the sole precursor for the multifunctional messenger molecule nitric oxide (NO) which, in certain human cancer cells, may influence tumor initiation, promotion, and progression, tumor-cell adhesion, apoptosis and angiogenesis (Lind 2004). Arginine plays also a vital role for cells lacking the enzyme argininosuccinate synthase, which is absent in many cancers (Dillon et al. 2004). Moreover, there is emerging evidence for tumor-associated up-regulation of the $ATB^{0,+}$ transporter and its expression was found to be markedly induced in colorectal (Gupta et al. 2005), cervical (Gupta et al. 2006) and estrogen receptor-positive breast cancer (Karunakaran et al. 2011). In this respect, cationic amino acid transport could be a promising target for oncologic imaging in terms of detection, prognosis and response to therapy monitoring of related tumors. Its potential though remains largely unexplored mainly because of the lack of well characterized imaging agents.

Our goal was to investigate the biological behavior of a [^{18}F]-labeled cationic amino acid derivative and to evaluate its potential for cancer imaging. To our knowledge, there is only one [^{18}F]-labeled basic amino acid analog under investigation as a potential PET probe for tumor imaging, the triazole derivative (*S*)-2-amino-3-[1-(2-[^{18}F]fluoroethyl)-1*H*-[1,2,3]triazol-4-yl]propanoic acid ([^{18}F]AFETP, Fig. 1) (McConathy et al. 2010; Solingapuram Sai et al. 2011). Biological evaluation showed that the uptake of [^{18}F]AFETP is mediated by several transport systems, both for neutral and cationic amino acids. This could be attributed to the weakly basic nature of the triazole moiety, probably rendering it neutral at physiological pH (Comer 2007) and possibly more basic amino acid derivatives are needed to efficiently target cationic amino acid transporters. For our purposes, we chose the successful PET tumor imaging agent and LAT1 substrate [^{18}F]FET as a lead structure for further derivatization towards a cationic surrogate. Therefore, tyrosine was combined with an aliphatic tertiary amine, namely diethanolmethylamine to give *O*-2((2-[^{18}F]fluoroethyl)methylamino)ethyl L-tyrosine ([^{18}F]FEMAET, Fig. 1). The presence of a tertiary nitrogen atom is expected to render [^{18}F]FEMAET cationic at physiological pH (Comer 2007; Smith and March 2007) which would most

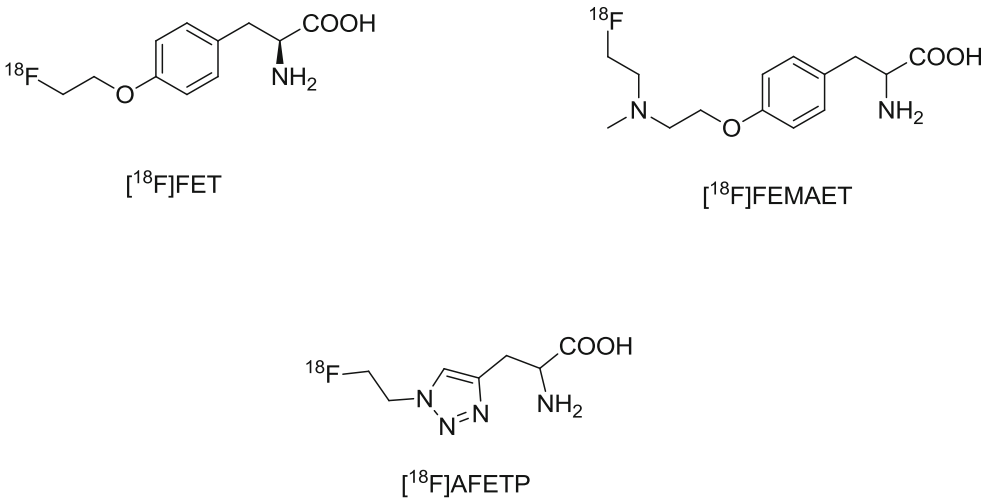

Fig. 1 Structures of [^{18}F]AFETP, [^{18}F]FET and its new cationic analog [^{18}F]FEMAET

probably exclude its uptake through the LAT or other neutral amino acid transporters.

In this work, we describe the synthesis, radiolabelling and preliminary biological evaluation of [^{18}F]FEMAET as a potential tracer for cationic amino acid uptake. To our knowledge, ATB$^{0,+}$ is the only transporter for cationic amino acids that is upregulated by cancer cells (Ganapathy et al. 2009; Nakanishi and Tamai 2011; Sloan and Mager 1999). We were, therefore, particularly interested to investigate possible implication of this transporter in the uptake of the new cationic tracer. For this reason, the small cell lung cancer NCI-H69 and the prostate cancer cell line PC-3 were chosen for the preliminary in vitro and in vivo studies, as they both express ATB$^{0,+}$ on the mRNA level (Müller et al. 2013).

Materials and methods

General

All reagents and starting materials were purchased from commercial suppliers and used without further purification. All solvents used for reactions were purchased as anhydrous grade from Acros Organics (puriss., dried over molecular sieves, $H_2O < 0.005$ %) and were used without further purification unless otherwise stated. Solvents for extractions, column chromatography and thin layer chromatography (TLC) were purchased as commercial grade. All non-aqueous reactions were performed under an argon atmosphere using flame-dried glassware and standard syringe/septa techniques. In general, reactions were magnetically stirred and monitored by TLC performed on Merck TLC glass sheets (silica gel 60 F_{254}). Spots were visualized with UV light ($\lambda = 254$ nm) or through staining with anisaldehyde solution or basic aq. $KMnO_4$ solution and subsequent heating. Chromatographic purification of products was performed using Fluka silica gel 60 for preparative column chromatography (particle size 40–63 μm). Reactions at 0 °C were carried out in an ice/water bath. Reactions at −78 °C were carried out in a dry ice/acetone bath. Nuclear magnetic resonance (NMR) spectra were recorded in $CDCl_3$ or CD_3OD on a Bruker Av-400 spectrometer at room temperature. The measured chemical shifts are reported in δ (ppm) and the residual signal of the solvent was used as the internal standard ($CDCl_3$ ^{1}H: $\delta = 7.26$ ppm, ^{13}C: $\delta = 77.0$ ppm, CD_3OD ^{1}H: $\delta = 3.31$ ppm, ^{13}C: $\delta = 49.15$ ppm). For the ^{19}F NMR spectra, $CFCl_3$ (=0.00 ppm) was used as the internal standard. All ^{13}C NMR spectra were measured with complete proton decoupling. Data of NMR spectra are reported as follows: *s* singlet, *d* doublet, *t* triplet, *q* quartet, *m* multiplet, *dd* doublet of doublets, *dt* doublet of triplets, *br* broad signal. The coupling constant *J* is reported in Hertz (Hz). Electrospray (ES) mass spectra (HRMS) were obtained with a Bruker's maXis (ESI-Qq-TOF-MS) spectrometer.

Analytical radio-HPLC was performed on an Agilent 1100 system equipped with multi-UV-wavelength and Raytest Gabi Star detectors and Gina Star software. A reverse phase column was used (LiChrospher® 100 RP-18 5 μm LiChroCART® 4 × 250 mm) with the following solvent system: H_2O (NH_4HCO_3 50 mM) (solvent A), acetonitrile (solvent B); flow 1 ml/min; 0–3 min: 5 % B, 3–15 min: 5–90 % B, 15–19 min: 90 % B, 19–20 min: 90–5 % B; UV = 254 nm. Semi-preparative purification of radiolabeled material was performed on a Merck-Hitachi L6200A system equipped with Knauer variable wavelength detector and an Emberline radiation detector using a reverse phase column (Phenomenex Luna C18, 10 × 250 mm, 5 μm) and a mobile phase consisting of the following system: H_2O (NH_4HCO_3 50 mM) (solvent A), acetonitrile (solvent B); flow 4 ml/min; 0–5 min: 5 % B, 5–10 min: 5–65 % B, 10–30 min: 65 % B; UV = 254 nm. For

reaction monitoring during radiosynthesis and for analysis of samples during radiometabolite and in vitro stability studies, a Waters Ultra-performance liquid chromatography (UPLC®) system was used with an Acquity UPLC BEH C18 column (2.1 × 50 mm, 1.7 μm, Waters) and an attached coincidence detector (FlowStar LBS13, Berthold). The mobile phase consisted of the following system: H_2O (NH_4HCO_3 50 mM) (solvent A), acetonitrile (solvent B); flow 0.6 ml/min; 0–0.3 min: 0 % B, 0.3–2.2 min: 0–70 % B, 2.2–2.7 min: 70 % B, 2.7–2.90 min: 70–0 % B; 2.90–3.00 min 0 %B; UV = 254 nm. Specific activity was calculated by comparing ultraviolet peak intensity of final formulated products with calibration curves of corresponding non-radioactive standards of known concentrations.

Chemistry

*2-((2-Hydroxyethyl)(methyl)amino)ethyl acetate (**1**)*

To a solution of *N*-methyldiethanolamine (9.97 g, 83.69 mmol) in ethyl acetate (20 ml), acetic anhydride (4.32 g, 42.40 mmol) was added dropwise at 0 °C. The reaction mixture was then allowed to reach room temperature and was stirred for 3 h. After this time, the reaction mixture was diluted with ethyl acetate and washed three times with saturated $NaHCO_3$ (aq.) solution, followed by water and brine. The combined organic phases were dried over sodium sulfate, filtered and concentrated. The crude product was purified by flash column chromatography on silica gel (dichloromethane/methanol = 93:7) to afford (**1**) (2.26 g, 33 %) as a clear oil. ^{1}H NMR ($CDCl_3$, 400 MHz) δ 2.07 (s, 3H, C*H*$_3$(C=O)O), 2.37 (s, 3H, C*H*$_3$N), 2.64 (t, J = 5.4 Hz, 2H, HOCH$_2$C*H*$_2$N), 2.75 (t, J = 5.7 Hz, 2H, CH$_3$C(=O)OCH$_2$C*H*$_2$N), 3.41 (br, 1H, O*H*), 3.61 (t, J = 5.4 Hz, 2H, HOC*H*$_2$CH$_2$N), 4.20 (t, J = 5.7 Hz, 2H, CH$_3$C(=O)OC*H*$_2$CH$_2$N). ^{13}C NMR ($CDCl_3$, 100 MHz) δ 21.1, 42.2, 55.8, 58.5, 59.0, 62.1, 171.2. ESI-QTOF MS m/z calculated for $C_7H_{16}NO_3$ $[M+H]^+$ 162.1121, measured 162.1121.

*Tert-butyl 2-((tert-butoxycarbonyl)amino)-3-(4-hydroxyphenyl) propanoate (**2**)*

To a mixture of tyrosine tert-butyl ester (1.76 g, 7.43 mmol) and $NaHCO_3$ (1.71 g, 20.39 mmol) in DMF (14 ml), di-tert-butyl dicarbonate (1.50 g, 6.86 mmol) was added at 0 °C. After 10 min, the reaction mixture was allowed to reach room temperature and the suspension was stirred for 40 h. After this time, the reaction mixture was diluted with ethyl acetate and washed four times with water and once brine then dried over magnesium sulfate, filtered and evaporated to dryness under reduced pressure. The residue was purified with flash column chromatography on silica gel (hexane/ethyl acetate = 7/3) to afford **2** (2.15 g, 93 %) as a white solid. ^{1}H NMR ($CDCl_3$, 400 MHz) δ 1.41 (s, 9H, C(C*H*$_3$)$_3$), 1.42 (s, 9H, C(C*H*$_3$)$_3$), 2.91–3.04 (m, 2H, ArC*H*$_2$CH), 4.40 (q, J_1 = 8.2 Hz and J_2 = 6.2 Hz, 1H, ArCH$_2$C*H*), 5.00 (d, J = 8.2 Hz, 1H, N*H*Boc), 5.36 (s, 1H, ArO*H*), 6.73 (d, J = 8.3 Hz, 2H, Ar*H*), 7.02 (d, J = 8.3 Hz, 2H, Ar*H*). ^{13}C NMR ($CDCl_3$, 100 MHz) δ 28.1, 28.5, 37.9, 55.2, 80.0, 82.3, 115.4, 128.5, 130.8, 154.9, 155.4, 171.3.ESI-QTOF MS m/z calculated for $C_{18}H_{28}NO_5$ $[M+H]^+$ 338.1962, measured 338.1961.

*Tert-butyl3-(4-(2-((2-acetoxyethyl)(methyl)amino)ethoxy)phenyl)-2-((tertbutoxycarbonyl)amino)-propanoate (**3**)*

Triphenylphosphine (3.27 g, 12.46 mmol) was added to a mixture of compounds **1** (2.00 g, 12.41 mmol) and **2** (4.21 g, 12.46 mmol), dissolved in tetrahydrofuran (26 ml). To this mixture, a solution of diethyl azodicarboxylate (DEAD) (2.18 g, 12.51 mmol) in tetrahydrofuran (14 ml) was added dropwise at room temperature within 15 min. The reaction mixture was stirred for 63 h and then concentrated on a rotary evaporator and taken up in a mixture of diethyl ether and ethyl acetate. The mixture was washed three times with 0.2 M HCl. The combined aqueous phases were washed twice with diethyl ether and turned basic by adding solid $NaHCO_3$ and then extracted three times with ethyl acetate. The combined extracts were washed once with brine, dried over sodium sulfate, filtered and concentrated to dryness. The crude product was purified by flash column chromatography on silica gel (hexane/ethyl acetate = 5/5, changing gradually to 4/6 and 4/6 with Et_3N 1 %) to afford **3** (4.11 g, 68 %) as a colorless clear oil.^{1}H NMR ($CDCl_3$, 400 MHz) δ 1.41 (s, 9H, C(C*H*$_3$)$_3$), 1.42 (s, 9H, C(C*H*$_3$)$_3$), 2.05 (s, 3H,C*H*$_3$C(=O)O), 2.41 (s, 3H, C*H*$_3$N), 2.77 (t, J = 5.8 Hz, 2H, CH$_3$C(=O)OCH$_2$C*H*$_2$N), 2.86 (t, J = 5.8 Hz, 2H, ArOCH$_2$C*H*$_2$N), 2.94–3.04 (m, 2H, ArC*H*$_2$CH), 4.04 (t, J = 5.8 Hz, 2H, ArOC*H*$_2$CH$_2$N), 4.19 (t, J = 5.8 Hz, 2H, CH$_3$C(=O)OC*H*$_2$CH$_2$N), 4.40 (q, J_1 = 8.0 Hz and J_2 = 6.0 Hz, 1H, ArCH$_2$C*H*), 4.95 (d, J = 8.0 Hz, 1H, N*H*Boc), 6.82 (d, J = 8.6 Hz, 2H, Ar*H*), 7.07 (d, J = 8.6 Hz, 2H, Ar*H*).^{13}C NMR ($CDCl_3$, 100 MHz) δ 21.2, 28.1, 28.5, 37.3, 43.3, 55.1, 56.2, 56.6, 62.4, 66.2, 79.8, 82.2, 114.6, 128.7, 130.7, 155.3, 157.9, 171.2, 171.3. ESI-QTOF MS m/z calculated for $C_{25}H_{41}N_2O_7$ $[M+H]^+$ 481.2908, measured 481.2913.

*Tert-butyl-2-((tert-butoxycarbonyl)amino)-3-(4-(2-((2-hydroxy-ethyl)(methyl)amino)ethoxy)phenyl)-propanoate (**4**)*

To a stirred solution of compound **3** (4.28 g, 8.90 mmol) in methanol (36 ml), potassium cyanide (0.29 g, 4.46 mmol) was added at room temperature. The reaction mixture was

stirred overnight and then evaporated to dryness under reduced pressure. The crude product was dissolved in dichloromethane and filtered through a short pad of silica gel to afford **4** (3.72 g, 95 %) as a clear oil. ^{1}H NMR ($CDCl_3$, 400 MHz) δ 1.41 (s, 9H, C(CH_3)$_3$), 1.42 (s, 9H, C(CH_3)$_3$), 2.38 (s, 3H,CH_3N), 2.65 (t, J = 5.2 Hz, 2H, HOCH$_2$CH_2N), 2.86 (t, J = 5.6 Hz, 2H, ArOCH$_2$CH_2N), 2.95-3.05 (m, 2H, ArCH_2CH), 3.60 (t, J = 5.2 Hz, 2H, HOCH_2CH$_2$N), 4.03 (t, J = 5.6 Hz, 2H, ArOCH_2CH$_2$N), 4.40 (q, J_1 = 7.9 Hz and J_2 = 6.3 Hz, 1H, ArCH$_2$CH), 4.96 (d, J = 7.9 Hz, 1H, NHBoc), 6.82 (d, J = 8.6 Hz, 2H, ArH), 7.07 (d, J = 8.6 Hz, 2H, ArH).^{13}C NMR ($CDCl_3$, 100 MHz) δ 28.1, 28.4, 37.7, 42.5, 55.0, 56.3, 58.7, 59.2, 66.1, 79.7,82.1, 114.5, 128.7, 130.7, 155.2, 157.8, 171.1.Varian HiResMALDI MS m/z calculated for $C_{23}H_{39}N_2O_6$ $[M+H]^+$ 439.2803, measured 439.2807.

*Tert-butyl-2-((tert-butoxycarbonyl)amino)-3-(4-(2-((2-chloroethyl)(methyl)amino)ethoxy)phenyl)-propanoate (**5**)*

A solution of methanesulfonyl chloride (130 mg, 1.14 mmol) in dichloromethane (1 ml) was added dropwise within 10 min to a solution of compound **4** (416 mg, 0.95 mmol) and triethylamine (259 mg, 2.56 mmol) in dichloromethane (5 ml) at −40 °C. The reaction mixture was left to stir overnight while the temperature reached 10 °C. The mixture was diluted with dichloromethane, washed once with 5 % $NaHCO_3$ solution, water and brine, dried over sodium sulfate, filtered and evaporated to dryness. The crude was purified by flash column chromatography (hexane/ethyl acetate/triethylamine 7:3:0.1) to afford **5** (270 mg, 62 %) as a clear oil.^{1}H NMR ($CDCl_3$, 400 MHz) δ 1.41 (s, 9H, C(CH_3)$_3$), 1.42 (s, 9H, C(CH_3)$_3$), 2.42 (s, 3H, CH_3N), 2.83–2.91 (m, 4H, ClCH$_2$CH_2N and ArOCH$_2$CH_2N), 2.94–3.03 (br, 2H, ArCH_2CH), 3.58 (t, J = 7.0 Hz, 2H, ClCH_2CH$_2$N), 4.04 (t, J = 5.8 Hz, 2H, ArOCH_2CH$_2$N), 4.40 (q, J_1 = 7.7 Hz and J_2 = 6.1 Hz, 1H, ArCH$_2$CH), 4.96 (d, J = 7.7 Hz, 1H,NHBoc), 6.82 (d, J = 8.4 Hz, 2H, ArH), 7.07 (d, J = 8.5 Hz, 2H, ArH).^{13}C NMR ($CDCl_3$, 100 MHz) δ 28.0, 28.4, 37.6, 41.6, 43.0, 55.0, 56.3, 59.4, 66.2, 79.6,82.0, 114.5, 128.4, 130.6, 155.1, 157.7, 171.1. ESI-QTOF MS m/z calculated for $C_{23}H_{38}ClN_2O_5$ $[M+H]^+$ 457.2464, measured 457.2463.

*Tert-butyl-3-(4-(2-((2-bromoethyl)(methyl) amino)ethoxy)phenyl)-2-(tert-butoxycarbonyl)amino)-propanoate (**6**)*

Triphenylphosphine (183.4 mg, 0.70 mmol) was added to an ice-cooled solution of **4** (250.7 mg, 0.57 mmol) in DCM (2.8 ml) and the solution was stirred for 15 min. Under protection from light, CBr_4 (288.3 mg, 0.869 mmol) was then added portion wise. After stirring for 1 h at 0 °C, the reaction mixture was allowed to reach room temperature where it was stirred for an additional hour. The reaction mixture was then evaporated to dryness under reduced pressure and the crude product was purified by flash column chromatography on silica gel (hexane/ethyl acetate = 7/3) to afford **6** (186.4 mg, 65 %) as a clear colorless oil. ^{1}H NMR ($CDCl_3$, 400 MHz) 1.41 (s, 9H, C(CH_3)$_3$), 1.42 (s, 9H, C(CH_3)$_3$), 2.42 (s, 3H, CH_3N), 2.88 (t, J = 5.7 Hz, 2H, ArOCH$_2$CH_2N), 2.93 (t, J = 7.6 Hz, 2H, BrCH$_2$CH_2N), 2.96–3.02 (br, 2H, ArCH_2CH), 3.43 (t, J = 7.6 Hz, 2H, BrCH_2CH$_2$N), 4.05 (t, J = 5.7 Hz, 2H, ArOCH_2CH$_2$N), 4.40 (q, J_1 = 7.9 Hz and J_2 = 6.1 Hz, 1H, ArCH$_2$CH), 4.96 (d, J = 7.9 Hz, 1H, NHBoc), 6.82 (d, J = 8.6 Hz, 2H, ArH), 7.07 (d, J = 8.7 Hz, 2H, ArH). ^{13}C NMR ($CDCl_3$, 100 MHz) 28.1, 28.5, 29.8, 37.7, 42.9, 55.1, 56.2, 59.5, 66.2, 79.7,82.1, 114.6, 128.7, 130.7, 155.2, 157.8, 171.2. ESI-QTOF MS m/z calculated for $C_{23}H_{38}BrN_2O_5$ $[M+H]^+$ 501.1959, measured 501.1953.

*Tert-butyl-2-((tert-butoxycarbonyl)amino)-3-(4-(2-((2-iodoethyl)(methyl)amino)ethoxy)phenyl)-propanoate (**7**)*

Iodine (276.1 mg, 1.09 mmol) was added to a solution of triphenylphosphine (286.4 mg, 1.09 mmol) and *N*-ethyldiisopropylamine (DIPEA) (163.2 mg, 1.26 mmol) in dichloromethane (4.6 ml) at 0 °C. Under strict exclusion of light, a solution of compound **4** (396 mg, 0.9 mmol) in dichloromethane (2.6 ml) was added dropwise. After 10 min of stirring at 0 °C, the reaction mixture was allowed to reach room temperature and stirred for 4 h. The solvent was then removed with a stream of argon and the crude was purified by flash column chromatography on silica gel (hexane/ethyl acetate = 7.5/2.5) to afford **7** (304.2 mg, 61 %) as a yellowish oil. ^{1}H NMR ($CDCl_3$, 400 MHz) δ 1.41 (s, 9H, C(CH_3)$_3$), 1.42 (s, 9H, C(CH_3)$_3$), 2.40 (s, 3H,CH_3N), 2.84–2.92 (m, 4H, ICH$_2$CH_2N and ArOCH$_2$CH_2N), 2.95–3.03 (br, 2H, ArCH_2CH), 3.22 (t, J = 7.8 Hz, 2H, ICH_2CH$_2$N), 4.05 (t, J = 5.7 Hz, 2H, ArOCH_2CH$_2$N), 4.40 (q, J_1 = 7.6 Hz and J_2 = 6.0 Hz, 1H, ArCH$_2$CH), 4.96 (d, J = 7.6 Hz, 1H, NHBoc), 6.82 (d, J = 8.6 Hz, 2H, ArH), 7.07 (d, J = 8.6 Hz, 2H, ArH). ^{13}C NMR ($CDCl_3$, 100 MHz) δ 28.1, 28.5, 37.7, 42.5, 55.1, 55.8, 60.5, 66.3, 79.7,82.1, 114.6, 128.5, 130.7, 155.3, 157.8, 171.2. ESI-QTOF MS m/z calculated for $C_{23}H_{38}IN_2O_5$ $[M+H]^+$ 549.1820, measured 549.1831. *Note* Since the compound is rather unstable, spectroscopic properties were measured without any delays and by taking related precautions.

*Tert-butyl-2-((tert-butoxycarbonyl)amino)-3-(4-(2-((2-fluoroethyl)(methyl)amino)ethoxy)phenyl)-propanoate (**8**)*

Method A Via fluorination of the iodo compound **7**. To a solution of compound **7** (304.2 mg, 0.56 mmol) in

tetrahydrofuran (5.8 ml), AgF (93.6 mg, 0.74 mmol) was added. The solution was stirred for 21 h at room temperature under exclusion of light. After the reaction was complete, the reaction mixture was filtered through a pad of Celite and washed with ethyl acetate. The filtrate and washings were combined and the solvent was removed under reduced pressure. The crude product was purified by flash column chromatography on silica gel (hexane/ethyl acetate = 5/5) to afford **8** (105.7 mg, 43 %) as a clear oil. ^{1}H NMR ($CDCl_3$, 400 MHz) δ 1.41 (s, 9H, $C(CH_3)_3$), 1.42 (s, 9H, $C(CH_3)_3$), 2.44 (s,3H, CH_3N), 2.81 (t, $J = 5.0$ Hz, 1H, FCH_2CH_2N), 2.85–2.92 (m, 3H, $ArOCH_2CH_2N$ and FCH_2CH_2N (unresolved J because of overlapping), 2.95–3.03 (br, 2H, $ArCH_2CH$), 4.06 (t, $J = 5.9$ Hz, 2H, $ArOCH_2CH_2N$), 4.40 (q, $J_1 = 7.7$ Hz and $J_2 = 6.1$ Hz, 1H, $ArCH_2CH$), 4.51 and 4.62 (dt, $^{2}J_{H–F} = 47.5$ Hz and $^{3}J_{H–H} = 5.0$ Hz, 2H, FCH_2CH_2N), 4.96 (d, $J = 7.7$ Hz, 1H,NHBoc), 6.82 (d, $J = 8.5$ Hz, 2H, ArH), 7.07 (d, $J = 8.6$ Hz, 2H, ArH). ^{13}C NMR ($CDCl_3$, 100 MHz) δ 28.1, 28.4, 37.7, 43.3, 55.1, 56.6, 57.7 (d, $^{2}J_{C–F} = 19.9$ Hz), 66.3, 79.7, 82.0, 82.4 (d, $^{1}J_{C-F} = 167.7$ Hz), 114.6, 128.7, 130.6, 155.3, 157.9, 171.2. ^{19}F NMR ($CDCl_3$, 376 MHz) δ (−219.63)–(−219.18) (m). ESI-QTOF MS m/z calculated for $C_{23}H_{38}FN_2O_5$ $[M+H]^+$ 441.2759, measured 441.2758.

Method B Via direct fluorination of the alcohol **4**. A solution of compound **4** (246.1 mg, 0.56 mmol) and *N*-ethyldiisopropylamine (DIPEA) (259.7 mg, 2.01 mmol) in dichloromethane (6.2 ml) was added dropwise, within 15 min, to a solution of diethylaminosulfurtrifluoride (DAST) (315.8 mg, 1.96 mmol) in dichloromethane (5.8 ml) at −78 °C. After stirring for 15 min at that temperature, the reaction was taken out of the cooling bath and stirred for 3 h at room temperature. The reaction mixture was then quenched with saturated $NaHCO_3$ (aq.) solution at 0 °C. The mixture was diluted with ethyl acetate and washed three times with saturated $NaHCO_3$ (aq.) solution. The organic phase was then washed once with water and then brine, dried over Na_2SO_4, filtered and evaporated. The crude product was purified by flash column chromatography on silica gel (hexane/ethyl acetate 5:5) to afford **8** (70.8 mg, 29 %) as a clear oil. NMR analysis showed an identical spectrum as in the case of method A.

*2-amino-3-(4-(2-((2-fluoroethyl)(methyl)amino)ethoxy)phenyl) propanoic acid (FEMAET) (**9**)*

Trifluoroacetic acid (1.31 g, 11.49 mmol) was added dropwise to a solution of **8** (83.8 mg, 0.19 mmol) in dichloromethane (1 ml) cooled at 0 °C. After the addition, the reaction was allowed to reach room temperature and stirred for 16 h. Removal of the volatiles under reduced pressure, afforded FEMAET as the TFA salt (94.3 mg, 97 %). ^{1}H NMR (CD_3OD, 400 MHz) δ 3.06 (s, 3H, CH_3N), 3.12 (dd, $^{2}J_1 = 14.8$ Hz and $^{3}J_2 = 7.5$ Hz, 1H, $ArCH_2CH$), 3.25 (dd, $^{2}J_{H–H} = 14.8$ Hz and $^{3}J_{H–H} = 5.7$ Hz, 1H, $ArCH_2CH$), 3.64 (br, 1H, FCH_2-CH_2N), 3.71 (br, 3H, $ArOCH_2CH_2N$ and FCH_2CH_2N), 4.20 (dd, $J_1 = 7.5$ Hz and $J_2 = 5.8$ Hz, 1H, $ArCH_2CH$), 4.39 (t, $J = 4.9$ Hz, 2H, $ArOCH_2CH_2N$), 4.83 and 4.95 (dt, $^{2}J_{H–F} = 47.2$ Hz and $^{3}J_{H–H} = 4.5$ Hz, 2H, FCH_2CH_2N), 7.02 (d, $J = 8.7$ Hz, 2H, ArH), 7.27 (d, $J = 8.7$ Hz, 2H, ArH). ^{13}C NMR (CD_3OD, 100 MHz) δ 36.6, 42.0, 55.2, 56.7, 57.5 (d, $^{2}J_{C–F} = 19.6$ Hz), 63.2,79.2 (d, $^{1}J_{C–F} = 168.8$ Hz), 116.3, 129.0, 131.9, 158.7, 171.3. ^{19}F NMR (CD_3OD, 376 MHz) δ (−223.43)–(−222.98) (m). Varian HiResMALDI MS m/z calculated for $C_{14}H_{22}FN_2O_3$ $[M+H]^+$ 285.1609, measured 285.1608.

Radiosynthesis of [^{18}F]FEMAET

The conversion of **5** to [^{18}F]-FEMAET was achieved via nucleophilic substitution with [^{18}F]-fluoride followed by Boc-deprotection. [^{18}F]-fluoride was obtained via the ^{18}O(p,n) ^{18}F reaction using 98 % enriched ^{18}O-water. $^{18}F^-$ was trapped on a light QMA cartridge (Waters), which was preconditioned with 0.5 M K_2CO_3 (5 ml) and water (5 ml). 1 ml Kryptofix $K_{2.2.2}$ solution [Kryptofix $K_{2.2.2}$: 2.5 mg, K_2CO_3: 0.5 mg in MeCN/water (2.3:1)] was used for the elution of $^{18}F^-$ from the cartridge. The solvents were evaporated at 110 °C under vacuum with a slight inflow of nitrogen gas. After addition of acetonitrile (1 ml), azeotropic drying was carried out. This procedure was repeated twice to afford dry [^{18}F]KF-$K_{2.2.2}$ complex. A solution of chloride **5** (5 mg in 300 µl dry DMSO) was added to the dried [^{18}F]KF-$K_{2.2.2}$ complex. The reaction mixture was heated at 100 °C for 10 min, followed by the addition of a 1:1 solution of MeCN:NH_4HCO_3 (50 mM) (2 ml). Purification was performed by semi-preparative HPLC, with [^{18}F] **8** eluting at about 21 min which was collected in a vial containing 40 ml of water. The product was trapped on a C18 light SepPak cartridge (Waters), which was preconditioned with ethanol (5 ml) and water (5 ml). After washing the cartridge with 10 ml of water for removal of traces of acetonitrile, the product was eluted with 1 ml of acetone. The solvent was removed under reduced pressure at 80 °C and then TFA (0.7 ml) was added and the solution was heated at 80 °C for 10 min. TFA was then removed under a flow of N_2 and the residue was azeotroped with 1 ml of ethyl acetate at 80 °C to remove traces of TFA. For the final formulation, the radiolabeled compound was dissolved in 1 ml PBS 0.1 M (with 5 % EtOH) and filtered through a sterile filter. Final pH was approximately 7. Identification of [^{18}F]FEMAET was confirmed by co-injection with reference **9**. Chemical and radiochemical

purity were determined by analytical HPLC; $t_R = 9.30$ min for [^{18}F]FEMAET. The radiochemical purity was always >99 %. [^{18}F]FET was obtained from a routine clinical production from the University Hospital Zürich, Switzerland.

In vitro cell uptake studies

For [^{18}F]FDOPA efflux experiments, cultures of PC-3 cells (American Type Culture Collection) were incubated with 20 kBq [^{18}F]FDOPA from a routine production for clinical use (University Hospital Zürich, Switzerland). After 1 h, cells were washed twice with EBSS before 400 µl EBSS containing 100 µM FEMAET in form of the TFA salt, pH adjusted to 7.4, was added to each well (time zero). The plates were incubated at the indicated temperature on a shaker at 25 rpm and wells were washed twice with ice-cold incubation solution at the indicated time points, detached with trypsin/EDTA (Invitrogen) and radioactivity was quantified in a gamma counter (Perkin Elmer Wizard 1480). Cell viability was confirmed at the end of the incubation with trypan blue staining.

In vitro cell uptake of [^{18}F]FEMAET was studied as previously described (Krämer et al. 2012). NCI-H69 cells (German Collection of Microorganisms and Cell Cultures, Cell Lines Service) were cultured in plastic tubes according to the supplier's protocol. Cells were sub-cultured the day before the transport experiments. Before the uptake assay, cells were washed twice and incubated with Earle's balanced salt solution containing Ca^{2+} and Mg^{2+} for 1 h at 37 °C to deplete intracellular amino acids (EBSS, Invitrogen). At time zero, 20 MBq [^{18}F]FEMAET was added to each tube and the cells were incubated at 37 °C at 25 rpm. At the indicated time points, cells were washed twice with ice-cold incubation solution, pelleted and radioactivity was determined in a gamma counter. For protein quantification, cells were lysed with 2 % sodium dodecyl sulfate and analyzed with the DC Protein Assay (Bio-Rad) and bovine serum albumin as standard.

In vitro metabolism

FEMAET was added at a final concentration of ~1 µM to a mixture of 50 µL NADPH regenerating system A (BD Biosciences), 10 µl NADPH regenerating system B (BD Biosciences), 200 µl TRIS buffer 375 mM and water in a total volume of 975 µl at 37 °C. At time 0, 25 µl human liver microsomes (BD Biosciences, 20 mg protein per ml) were added and the mix was incubated at 37 °C and 600 rpm for 60 min. Aliquots of 100 µl were removed at various time points and added to 100 µl ice-cold methanol to stop enzymatic activity and precipitate proteins. The samples were centrifuged and the supernatants filtered into HPLC vials. Samples were analyzed with an analytical Hitachi HPLC system (consisting of an autosampler L-2200, pump L-2130, column oven L-2300, fluorescence detector L-2480, UV detector L-2420) and a LiChroCART® 250-4 HPLC-cartridge (Lichrospher® 100, RP-18e, 5 µm, 28 °C). The mobile phase consisted of acetonitrile (solvent A) and 0.1 % trifluoroacetic acid in water (solvent B); flow 1.0 ml/min; 0–3 min: 95 % B, 3–13 min 95–85 % B, 13–18 min 80–20 % B, 18–21 min 20 % B, 21–22 min 20–95 % B, 22–30 min 95 % B. FEMAET was quantified with a fluorescence detector (excitation 260 nm, emission 300 nm). The experiment was performed in triplicate. Enzymatic activity was confirmed with 2 µM testosterone instead of FEMAET according to the supplier's protocol. Testosterone samples were run on a Water Spherisorb® ODS2 analytical cartridge (250 × 4.6 mm, 5 µm, 40 °C) with sodium phosphate buffer (0.1 mM, pH6), methanol, acetonitrile (50:38.5:11.5 (v/v/v)) at a flow rate of 1.2 ml/min. Testosterone and its metabolites were detected at 242 nm.

In vivo metabolism

[^{18}F]FEMAET (23 and 43 MBq, respectively) was injected into two NMRI nu/nu mice via tail vein. The mice were killed by decapitation under isoflurane anesthesia 60 min after tracer application and blood and urine were collected. Plasma was separated from the blood samples by centrifugation and plasma and urine were extracted with ice-cold acetonitrile at 1:1 volume ratios. The organic phases were spotted on two silica gel TLC plates each (aluminum sheets, silica gel 60, Merck Millipore) together with a trace of [^{18}F]FEMAET and developed in $CHCl_3$/MeOH/acetic acid/water, 60/50/1/4 and $CHCl_3$/MeOH/NH_3, 55/44/4.1, respectively. Radioactivity was detected with a Canberra-Packard Instant Imager (Perkin Elmer, Watford, UK).

In vivo PET studies

In vivo experiments were approved by the Veterinary Office of the Canton Zürich and were conducted in accordance with the Swiss Animal Welfare legislation. Female NMRI nu/nu mice (Charles River, Sulzfeld, Germany) were inoculated at 6 weeks of age subcutaneously with 1×10^7 NCI-H69 cells in 100 µl PBS with Ca^{2+} and Mg^{2+} (Invitrogen; BP bioscience) on the right shoulder and 1 week later with the same cell number in matrigel (BD Biosciences) on the left shoulder. PET/CT scans were performed 2–5 weeks after inoculation, when the tumor volumes reached >0.025 cm^3. [^{18}F]FEMAET (5.6 MBq, 0.1 ml) or [^{18}F]FET (11.7 MBq, 0.1 ml) was injected into a lateral tail vein and anesthesia (2–3 % isoflurane in oxygen/air) was initiated 10 min before scan start.

Respiratory frequency and temperature were monitored and controlled as described previously (Honer et al. 2004). [^{18}F]FEMAET was scanned with a Vista eXplore PET/CT camera (Sedecal, Spain, axial field of view 4.8 cm) in static mode with two bed positions from 60 to 75 min p.i. for the anterior body part including the tumor and 75–90 min for the posterior body part. [^{18}F]FET was scanned in list mode, one bed position, from 30 to 120 min p.i. PET was followed by CT acquisition for anatomical orientation. PET data were reconstructed by 2-dimensional ordered-subsets expectation maximization and analyzed with PMOD 3.4 (PMOD, Zürich, Switzerland). Standardized uptake values (SUV) were calculated for regions of interest as the ratio of regional averaged Bq/cm^3 and injected radioactivity in Bq per g body weight. The [^{18}F]FET tumor-to-tissue ratio was highest from 60 to 75 min p.i., PET images were, therefore, prepared from averaged data during this time window.

Results and discussion

Chemistry

FEMAET was synthesized starting from commercially available tyrosine tert-butyl ester and diethanolmethylamine as depicted in Scheme 1. Diethanolmethylamine was first converted to the monoacetate **1** using acetic anhydride which was then coupled to L-tyrosine-*N*-Boc tert-butyl ester under Mitsunobu reaction conditions (DEAD/PPh_3) in THF yielding the key intermediate **3** in 68 % yield. Remarkably, the acetyl group in **3** proved quite resilient and initial attempts to deacetylate **3** using standard conditions such as K_2CO_3/MeOH or 1 M NaOH/MeOH failed. Nevertheless, treating a solution of this compound in MeOH with KCN as transesterification catalyst (Herzig et al. 1986) allowed complete conversion and afforded the free alcohol **4** in excellent yields. For the following step, it was originally planned to introduce a sulfonate as an efficient leaving group for the subsequent fluorination. However, mesylation of compound **4** afforded exclusively the chlorinated analog **5** in 72 % yield. This unexpected behavior has also been observed for other similar compounds in the literature (Bacherikov et al. 2005; Savle et al. 1998). It is suggested that this conversion occurs via spontaneous displacement of the sulfonate group by nitrogen (anchimeric assistance) with formation of the reactive intermediate aziridinium ion. Consequent collapse of the aziridinium ion pair to the more stable chloride then occurs, upon exchange of the tosylate counterion with chloride (Boeckman et al. 2011).

Since introduction of a sulfonate group was not possible, iodine was chosen as an efficient leaving group instead. The iodinated analog **7** was successfully synthesized via dehydroxylation—iodination reaction (Silhar et al. 2005). Choosing an appropriate base seems to be important since the conversion was more effective when using DIPEA instead of imidazole. The iodo compound **7** proved to be very sensitive to light and moisture so the reaction took place under strict exclusion of light and purification was performed without delays. Exchange of iodine to fluorine was accomplished using AgF as a source of fluorine yielding compound **8** in 43 % yield. To overcome the problems associated with the sensitivity of the iodinated compound, alcohol **4** was directly converted to **8** using DAST as fluorinating agent (Okuda et al. 2009), albeit in 29 % yield which is comparable to the overall yield of the conversion of **4**–**8** via the iodo compound. Finally, cleavage of the two tert-butyl groups with TFA yielded cleanly the final compound **9** (FEMAET). As it was already mentioned, the iodinated compound **7** is quite unstable, to a point which makes its use as a radiolabeling precursor rather impractical. For this reason, the analog brominated compound **6** was also synthesized from alcohol **4** using CBr_4/PPh_3, in hope to use this compound as an efficient radiolabeling precursor. Unfortunately, **6** also proved to be rather unstable as it was completely decomposed after storage at −25 °C within a short period of time. On the other hand, the chlorinated compound **5** remained unchanged under storage and it was thus decided to be used as a radiolabeling precursor, despite the chlorine atom being a poor leaving group.

Radiochemistry

[^{18}F]FEMAET was prepared via nucleophilic substitution of the chloride **5** with non-carrier-added [^{18}F]KF-$K_{2.2.2}$ complex in DMSO, followed by deprotection, as shown in Scheme 2. The fluorinated intermediate [^{18}F] **8** was purified by semi-HPLC purification, separating it efficiently from its chloro-precursor despite their very similar chemical properties. [^{18}F] **8** was recovered from the HPLC eluate using solid phase extraction with a C-18 light Sep-Pak cartridge. The activity was eluted with EtOH, dried and the intermediate was deprotected quantitatively using TFA followed by evaporation, providing [^{18}F]FEMAET in a radiochemically pure form not requiring further purification. For the final formulation, the residue was dissolved inPBS 0.1 M (with 5 % EtOH) and filtered through a sterile filter. Analytical samples after dose formulation of [^{18}F]FEMAET were stable for at least 4 h as assessed by HPLC analysis. In a typical experiment, a radiochemical yield of about 18 % (decay corrected) was achieved with a radiochemical purity ≥99 % in a total synthesis and formulation time of approximately 2 h. The specific activities for [^{18}F]FEMAET were in the range of 28–45 GBq/μmol at the end of synthesis. The total synthesis time from end of

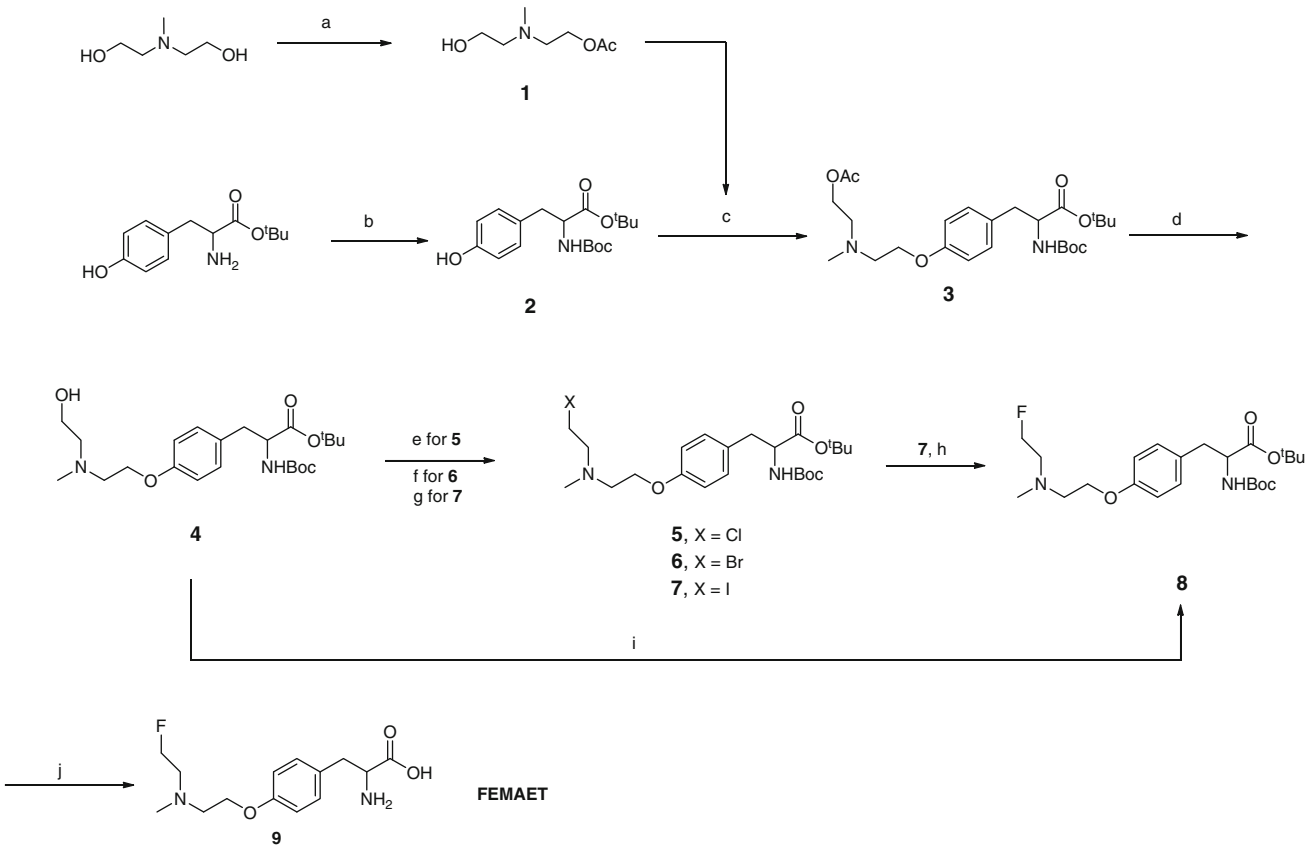

Scheme 1 Synthesis of FEMAET (**9**). Reagents and conditions: **a** acetic anhydride, AcOEt, 0 °C to room temperature, 3 h, 33 %; **b** Boc anhydride, $NaHCO_3$, DMF, 0 °C to room temperature, 40 h, 93 %; **c** DEAD, PPh_3, **1**, THF, room temperature, 64 h, 68 %; **d** KCN, MeOH, room temperature, 16 h, 95 %; **e** MsCl, Et_3N, DCM, −40° to 10 °C, 15 h, 62 %; **f** PPh_3, CBr_4, DCM, 0 °C to room temperature, 2 h, 65 %; **g** PPh_3, I_2, DIPEA, DCM, 0 °C to room temperature, 4 h, 61 %; **h** AgF, THF, room temperature, 21 h, 43 %; **i** DAST, DIPEA, DCM, −78 °C to room temperature, 3 h, 29 %; **j** TFA, DCM, 0 °C to room temperature, 16 h, quantitative

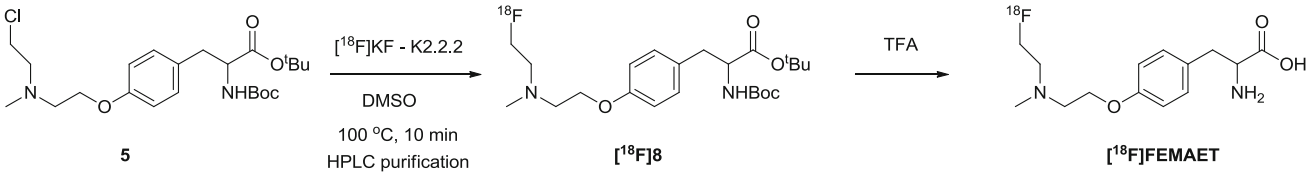

Scheme 2 Radiosynthesis of [^{18}F]FEMAET

bombardment was approximately 90 min. The identity of the radiolabelled compound was confirmed by co-injection with the reference compound **9**.

In vitro cell uptake

Cell uptake studies were performed with PC-3 prostate cancer and NCI-H69 small cell lung cancer cells. Both cell lines express $ATB^{0,+}$ on the mRNA level (Müller et al. 2013). Amino acid uptake into polarized cells is often directly or indirectly coupled to the efflux of other amino acids out of the cell (Wagner et al. 2001). Before establishing the radiosynthesis, we investigated whether FEMAET is able to enhance the efflux of preloaded [^{18}F]FDOPA, a substrate for LAT (Neels et al. 2008) from PC-3 cells. Addition of 100 µM FEMAET accelerated [^{18}F]FDOPA efflux at 37 °C (Fig. 2a) but not at 4 °C, indicating energy-dependent uptake of FEMAET into the cells with efflux of [^{18}F]FDOPA in compensation. However, the effect was weaker than that of the LAT substrate L-leucine (Krämer et al. 2012), which provoked depletion of [^{18}F]FDOPA within a few minutes at 37 and 4 °C under otherwise identical experimental conditions (Krämer et al. 2012). This excludes efficient transport of FEMAET by the obligatory exchange transporters LAT1 or LAT2.

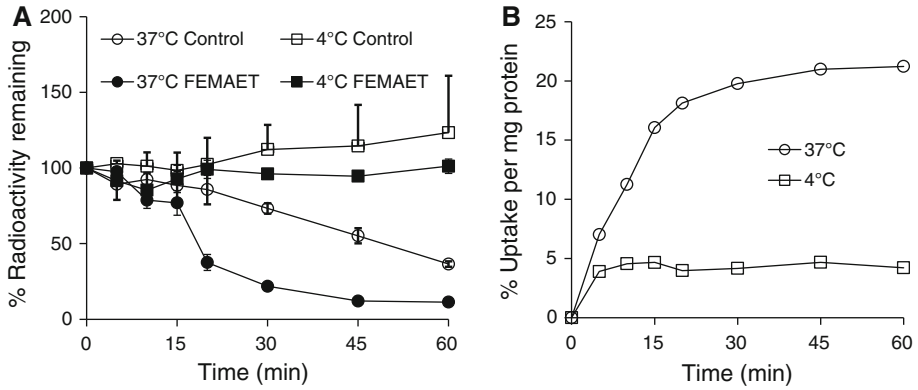

Fig. 2 Indirect and direct evidence of FEMAET uptake into tumor cells in vitro. **a** PC-3 cells were incubated with [^{18}F]FDOPA at 37 °C. After 60 min, the medium was replaced by 100 μM FEMAET (2 independent experiments, error bars show single values) or amino acid-free EBSS (4 independent experiments, mean and standard deviations) and [^{18}F]FDOPA remaining in the cells was determined at 37 and 4 °C. **b** Uptake of [^{18}F]FEMAET into NCI-H69 cells at 37 and 4 °C (one experiment each)

Consequently, we proceeded with the radiosynthesis of [^{18}F]FEMAET for further characterization. Uptake of [^{18}F]FEMAET in ATB$^{0,+}$-positive NCI-H69 cells is depicted in Fig. 2b. The new tracer efficiently accumulated in this cancer cell line and the uptake was strikingly dependent on the temperature, as already seen with the PC-3 cells, in agreement with an energy-dependent uptake mechanism.

Due to the presence of a tertiary amine on the side chain of [^{18}F]FEMAET, the tracer is positively charged at physiological pH with an expected pKa between 10 and 11 (Smith and March 2007). This most probably excludes its transport by neutral amino acid transport systems like LAT1 or ASCT2 which strictly carry neutral amino acids (Ganapathy et al. 2009; Nakanishi and Tamai 2011; Verrey et al. 2004). On the other hand, the energy dependency observed in the uptake of [^{18}F]FEMAET could indicate possible involvement of the concentrative ATB$^{0,+}$ as a transport mechanism since this is driven by the membrane potential, in particular Na^+ and Cl^- transmembrane gradients (Sloan and Mager 1999). Certainly, transport of cationic amino acids can also be mediated by several other cationic amino acid transporters (CAT, y^+L, $b^{0,+}$ AT) besides ATB$^{0,+}$. Nevertheless, these transport systems maintain basal cationic amino acid availability and only ATB$^{0,+}$ is able to concentrate amino acids intracellularly utilizing the membrane potential as energy source (Nakanishi and Tamai 2011). In any case, more studies are required to characterize the exact uptake mechanism of [^{18}F]FEMAET into cancer cells and healthy tissue.

In vitro and in vivo metabolism

Carbon atoms in α-position to ether oxygen atoms are generally good targets for oxygenation by cytochrome P450 monooxygenases (Testa and Kramer 2007). In the case of FEMAET, such a transformation would generate 2-((2-fluoroethyl)(methyl)amino)ethanol and tyrosine. In this respect, the stability of FEMAET in liver microsomes was tested in vitro by incubating the compound with human liver microsomes at 37 °C. Results indicated that FEMAET was stable without marked decomposition for 60 min; in particular, no tyrosine was formed. The metabolic stability of [^{18}F]FEMAET was also confirmed in vivo in healthy mice. TLC analysis of plasma showed only parent tracer but no metabolite 1 h after tracer application. Only traces of radiometabolites were detected in urine besides the parent tracer (data not shown).

PET imaging with NCI-H69 xenograft-bearing mice

Tumor accumulation of [^{18}F]FEMAET was evaluated by small animal PET with NCI-H69 xenograft-bearing mice. As shown in Fig. 3a, [^{18}F]FEMAET significantly accumulated in the NCI-H69 xenograft exhibiting good tumor visualization. No accumulation of radioactivity in bones was observed which suggests that [^{18}F]FEMAET does not defluorinate in vivo. Figure 3b shows a PET scan with [^{18}F]FET under similar conditions. The SUV ratios between xenografts and the neck were 2.1 and 2.6 for [^{18}F]FEMAET and [^{18}F]FET, respectively, demonstrating the good imaging potential of [^{18}F]FEMAET. Figure 3c, d shows the brain uptake of the two tyrosine analogs. Transport of large neutral amino acids across the blood–brain barrier is mediated by LAT1 (Hawkins et al. 2006; Boado et al. 1999). As expected, [^{18}F]FET radioactivity in brain was similar as in peripheral tissues (Wester et al. 1999). In contrast, brain levels of [^{18}F]FEMAET were significantly lower than in peripheral tissues. This would be expected for an ATB$^{0,+}$ substrate as the transporter is absent in brain (Sloan and Mager 1999). The cationic

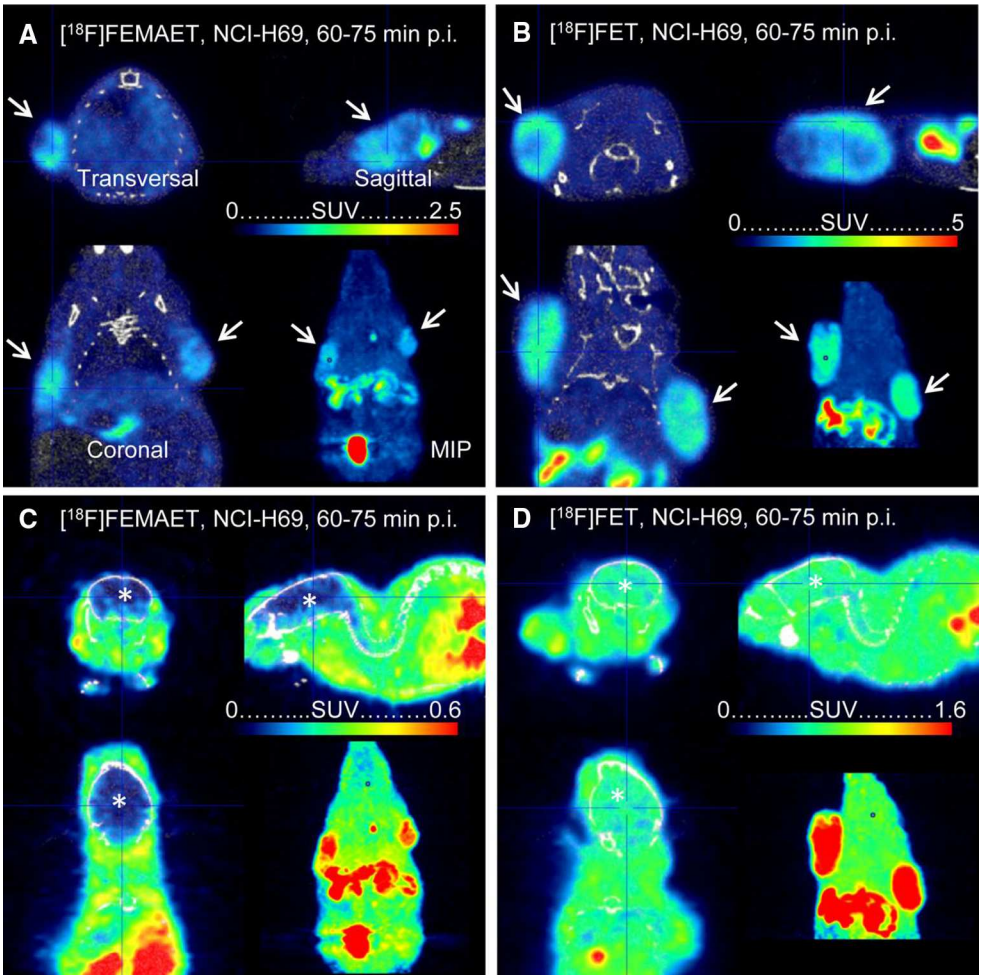

Fig. 3 PET/CT images of NCI-H69 xenograft-bearing mice with [^{18}F]FEMAET (**a**, **c**) and [^{18}F]FET (**b**, **d**). **a**, **b** Uptake into xenografts (*arrows*); **c**, **d** same scans as in (**a**) and (**b**), brain (*asterisk*) uptake. Injected doses were 5.6 MBq [^{18}F]FEMAET and 11.7 MBq [^{18}F]FET. *Color*, PET; *white/grey*, CT. SUV scale was chosen to have similar *background colors* in **a**, **b** and **c**, **d**, respectively (color figure online)

nature of [^{18}F]FEMAET is most probably excluding its transport by the system L amino acid transport.

Conclusion

In conclusion, our attempt to develop a novel [^{18}F]-labeled cationic amino acid derivative for tumor imaging has proved to be encouraging. [^{18}F]FEMAET, a cationic analog of the well-established [^{18}F]FET tracer, was prepared by convenient procedures with satisfactory radiochemical yield and specific activity. PET imaging in NCI-H69 tumor-bearing mice revealed good tumor visualization with tumor/peripheral tissues ratio in the range of neutral amino acid PET probes. This shows that, in principle, tumor imaging is possible with a cationic PET probe. In addition, the cationic nature of [^{18}F]FEMAET in combination with the preliminary biological evaluation suggests that the new tracer could be potentially a substrate for cationic amino acid transport. More importantly, there are indications that the concentrative transporter ATB$^{0,+}$ is possibly involved in [^{18}F]FEMAET transport. Such a feature would make [^{18}F]FEMAET an attractive PET probe for the imaging of malignant lesions that overexpress this transporter. Certainly more extensive biological assessment is needed to elucidate its exact uptake mechanism and provide solid proof about possible selectivity for the ATB$^{0,+}$ transporter. Further pharmacological characterization of this novel tracer is currently ongoing.

Acknowledgments We thank Claudia Keller for the excellent technical help in conducting in vitro and in vivo experiments.

Conflict of interest The authors declare that they have no conflict of interest.

References

Bacherikov VA, Chou TC, Dong HJ, Zhang X, Chen CH, Lin YW, Tsai TJ, Lee RZ, Liu LF, Su TL (2005) Potent antitumor 9-anilinoacridines bearing an alkylating *N*-mustard residue on the anilino ring: synthesis and biological activity. Bioorg Med Chem 13(12):3993–4006. doi:10.1016/j.bmc.2005.03.057

Beugnet A, Tee AR, Taylor PM, Proud CG (2003) Regulation of targets of mTOR (mammalian target of rapamycin) signalling by intracellular amino acid availability (vol 372, pg 555, 2003). Biochem J 373:999

Boado RJ, Li JY, Nagaya M, Zhang C, Pardridge WM (1999) Selective expression of the large neutral amino acid transporter at the blood-brain barrier. P Natl Acad Sci USA 96(21):12079–12084. doi:10.1073/pnas.96.21.12079

Boeckman RK Jr, Miller Y, Savage D, Summerton JE (2011) Total synthesis of a possible specific and effective acid-targeted cancer diagnostic, a camphor derived bis-*N*-oxide dimer. Tetrahedron Lett 52(17):2243–2245

Busch H, Davis JR, Honig GR, Anderson DC, Nair PV, Nyhan WL (1959) Uptake of a variety of amino acids into nuclear proteins of tumors and other tissues. Cancer Res 19(10):1030–1039

Closs EI (2002) Expression, regulation and function of carrier proteins for cationic amino acids. Curr Opin Nephrol Hy 11(1):99–107. doi:10.1097/00041552-200201000-00015

Closs EI, Boissel JP, Habermeier A, Rotmann A (2006) Structure and function of cationic amino acid transporters (CATs). J Membrane Biol 213(2):67–77. doi:10.1007/s00232-006-0875-7

Comer JEA (2007) Ionization constants and ionization profiles. In: Testa B, Van de Waterbeemd H (eds) Comprehensive Medicinal Chemistry II, vol 5. Elsevier, Amsterdam, pp 357–397

Dillon BJ, Prieto VG, Curley SA, Ensor CM, Holtsberg FW, Bomalaski JS, Clark MA (2004) Incidence and distribution of argininosuccinate synthetase deficiency in human cancers—a method for identifying cancers sensitive to arginine deprivation. Cancer 100(4):826–833. doi:10.1002/Cncr.20057

Fuchs BC, Bode BP (2005) Amino acid transporters ASCT2 and LAT1 in cancer: partners in crime? Semin Cancer Biol 15(4):254–266. doi:10.1016/j.semcancer.2005.04.005

Ganapathy V, Thangaraju M, Prasad PD (2009) Nutrient transporters in cancer: relevance to Warburg hypothesis and beyond. Pharmacol Therapeut 121(1):29–40. doi:10.1016/j.pharmthera.2008.09.005

Gupta N, Miyauchi S, Martindale RG, Herdman AV, Podolsky R, Miyake K, Mager S, Prasad PD, Ganapathy ME, Ganapathy V (2005) Upregulation of the amino acid transporter $ATB^{(0,+)}$ (SLC6A14) in colorectal cancer and metastasis in humans. Bba Mol Basis Dis 1741(1–2):215–223. doi:10.1016/j.bbadis.2005.04.002

Gupta N, Prasad PD, Ghamande S, Moore-Martin P, Herdman AV, Martindale RG, Podolsky R, Mager S, Ganapathy ME, Ganapathy V (2006) Up-regulation of the amino acid transporter $ATB^{(0,+)}$ (SLC6A14) in carcinoma of the cervix. Gynecol Oncol 100(1):8–13. doi:10.1016/j.ygyno.2005.08.016

Hawkins RA, O'Kane RL, Simpson IA, Vina JR (2006) Structure of the blood-brain barrier and its role in the transport of amino acids. J Nutr 136(1):218s–226s

Herzig J, Nudelman A, Gottlieb HE, Fischer B (1986) Studies in sugar chemistry 2. A simple method for *O*-deacylation of polyacylated sugars. J Org Chem 51(5):727–730

Honer M, Bruhlmeier M, Missimer J, Schubiger AP, Ametamey SM (2004) Dynamic imaging of striatal D-2 receptors in mice using quad-HIDAC PET. J Nucl Med 45(3):464–470

Kaim AH, Weber B, Kurrer MO, Westera G, Schweitzer A, Gottschalk J, von Schulthess GK, Buck A (2002) F-18-FDG and F-18-FET uptake in experimental soft tissue infection. Eur J Nucl Med Mol I 29(5):648–654. doi:10.1007/s00259-002-0780-y

Kanai Y, Fukasawa Y, Cha SH, Segawa H, Chairoungdua A, Kim DK, Matsuo H, Kim JY, Miyamoto K, Takeda E, Endou H (2000) Transport properties of a system y(+)L neutral and basic amino acid transporter—insights into the mechanisms of substrate recognition. J Biol Chem 275(27):20787–20793. doi:10.1074/jbc.M000634200

Karunakaran S, Ramachandran S, Coothankandaswamy V, Elangovan S, Babu E, Periyasamy-Thandavan S, Gurav A, Gnanaprakasam JP, Singh N, Schoenlein PV, Prasad PD, Thangaraju M, Ganapathy V (2011) SLC6A14 (ATB(0, +)) protein, a highly concentrative and broad specific amino acid transporter, is a novel and effective drug target for treatment of estrogen receptor-positive breast cancer. J Biol Chem 286(36):31830–31838. doi:10.1074/jbc.M111.229518

Kim DK, Ahn SG, Park JC, Kanai Y, Endou H, Yoon JH (2004) Expression of L-type amino acid transporter 1 (LAT1) and 4F2 heavy chain (4F2hc) in oral squamous cell carcinoma and its precusor lesions. Anticancer Res 24(3A):1671–1675

Kobayashi K, Ohnishi A, Promsuk J, Shimizu S, Kanai Y, Shiokawa Y, Nagane M (2008) Enhanced tumor growth elicited by L-type amino acid transporter 1 in human malignant glioma cells. Neurosurgery 62(2):493–503. doi:10.1227/01.Neu.0000255470.75752.02

Koopmans KP, Neels ON, Kema IP, Elsinga PH, Links TP, de Vries EGE, Jager PL (2009) Molecular imaging in neuroendocrine tumors: molecular uptake mechanisms and clinical results. Crit Rev Oncol Hemat 71(3):199–213. doi:10.1016/j.critrevonc.2009.02.009

Krämer SD, Mu L, Müller A, Keller C, Kuznetsova OF, Schweinsberg C, Franck D, Müller C, Ross TL, Schibli R, Ametamey SM (2012) 5-(2-18F-fluoroethoxy)-L-tryptophan as a substrate of system L transport for tumor imaging by PET. J Nucl Med 53(3):434–442. doi:10.2967/jnumed.111.096289

Langen KJ, Hamacher K, Weckesser M, Floeth F, Stoffels G, Bauer D, Coenen HH, Pauleit D (2006) *O*-(2-[(18)F]fluoroethyl)-L-tyrosine: uptake mechanisms and clinical applications. Nucl Med Biol 33(3):287–294. doi:10.1016/j.nuemedbio.2006.01.002

Lee TS, Ahn SH, Moon BS, Chun KS, Kang JH, Cheon GJ, Choi CW, Lim SM (2009) Comparison of F-18-FDG, F-18-FET and F-18-FLT for differentiation between tumor and inflammation in rats. Nucl Med Biol 36(6):681–686. doi:10.1016/j.nucmedbio.2009.03.009

Lind DS (2004) Arginine and cancer. J Nutr 134(10):2837s–2841s

McConathy J, Goodman MM (2008) Non-natural amino acids for tumor imaging using positron emission tomography and single photon emission computed tomography. Cancer Metast Rev 27(4):555–573. doi:10.1007/s10555-008-9154-7

McConathy J, Zhou D, Shockley SE, Jones LA, Griffin EA, Lee H, Adams SJ, Mach RH (2010) Click synthesis and biologic evaluation of (R)- and (S)-2-amino-3-[1-(2-[F-18]Fluoroethyl)-1H-[1,2,3]Triazol-4-yl]propanoic acid for brain tumor imaging with positron emission tomography. Mol Imaging 9(6):329–342. doi:10.2310/7290.2010.00025

McConathy J, Yu WP, Jarkas N, Seo W, Schuster DM, Goodman MM (2012) Radiohalogenated nonnatural amino acids as PET and SPECT tumor imaging agents. Med Res Rev 32(4):868–905. doi:10.1002/Med.20250

Müller A, Chiotellis A, Keller C, Ametamey SM, Schibli R, Mu L, Krämer SD (2013) Imaging tumour $ATB^{0,+}$ transport activity by PET with the cationic amino acid O-2((2-[^{18}F]fluoroethyl)methyl-amino)ethyltyrosine. Mol Imaging Biol. doi:10.1007/s11307-013-0711-2

Nakanishi T, Tamai I (2011) Solute carrier transporters as targets for drug delivery and pharmacological intervention for chemotherapy. J Pharm Sci Us 100(9):3731–3750. doi:10.1002/Jps.22576

Nawashiro H, Otani N, Shinomiya N, Fukui S, Ooigawa H, Shima K, Matsuo H, Kanai Y, Endou H (2006) L-type amino acid transporter 1 as a potential molecular target in human astrocytic tumors. Int J Cancer 119(3):484–492. doi:10.1002/Ijc.21866

Neels OC, Koopmans KP, Jager PL, Vercauteren L, van Waarde A, Doorduin J, Timmer-Bosscha H, Brouwers AH, de Vries EGE, Dierckx RAJO, Kema IP, Elsinga PH (2008) Manipulation of [C-11]-5-hydroxytryptophan and 6-[F-18]fluoro-3,4-dihydroxy-L-phenylalanine accumulation in neuroendocrine tumor cells. Cancer Res 68(17):7183–7190. doi:10.1158/0008-5472.Can-08-0095

Okuda K, Hirota T, Kingery DA, Nagasawa H (2009) Synthesis of a fluorine-substituted puromycin derivative for Bronsted studies of ribosomal-catalyzed peptide bond formation. J Org Chem 74(6):2609–2612. doi:10.1021/jo802611t

Plathow C, Weber WA (2008) Tumor cell metabolism imaging. J Nucl Med 49:43s–63s. doi:10.2967/jnumed.107.045930

Saier MH, Daniels GA, Boerner P, Lin J (1988) Neutral amino-acid transport-systems in animal-cells—potential targets of oncogene action and regulators of cellular growth. J Membrane Biol 104(1):1–20. doi:10.1007/Bf01871898

Savle PS, Medhekar RA, Kelley EL, May JG, Watkins SF, Fronczek FR, Quinn DM, Gandour RD (1998) Change in the mode of inhibition of acetylcholinesterase by (4-nitrophenyl)sulfonoxyl derivatives of conformationally constrained choline analogues. Chem Res Toxicol 11(1):19–25. doi:10.1021/tx970019o

Schoder H, Larson SM (2004) Positron emission tomography for prostate, bladder, and renal cancer. Semin Nucl Med 34(4):274–292. doi:10.1053/j.semnuclmed.2004.06.004

Shreve PD, Anzai Y, Wahl RL (1999) Pitfalls in oncologic diagnosis with FDG PET imaging: physiologic and benign variants. Radiographics 19(1):61–77

Silhar P, Pohl R, Votruba I, Hocek M (2005) The first synthesis and cytostatic activity of novel 6-(fluoromethyl)purine bases and nucleosides. Org Biomol Chem 3(16):3001–3007. doi:10.1039/b508122j

Sloan JL, Mager S (1999) Cloning and functional expression of a human Na^+ and Cl^- dependent neutral and cationic amino acid transporter B^{0+}. J Biol Chem 274(34):23740–23745. doi:10.1074/jbc.274.34.23740

Smith MB, March J (2007) March's advanced organic chemistry: reactions, mechanisms and structure, 6th edn. Wiley Interscience, Hoboken, pp 355–394

Solingapuram Sai K, Huang CF, Yuan LY, Zhou D, Garbow J, Rich K, Mach R, McConathy J (2011) Comparison of the non-natural amino acid, (S)-[F-18]AFETP, and [F-18]FDG for brain tumor imaging in the mouse DBT model of glioma. J Label Compd Radiopharm 54:S33–S33

Sundin A, Eriksson B, Bergstrom M, Langstrom B, Oberg K, Orlefors H (2004) PET in the diagnosis of neuroendocrine tumors. Ann Ny Acad Sci 1014:246–257. doi:10.1196/annals.1294.027

Sundin A, Garske U, Orlefors H (2007) Nuclear imaging of neuroendocrine tumours. Best Pract Res Cl En 21(1):69–85. doi:10.1016/j.beem.2006.12.003

Tamai S, Masuda H, Ishii Y, Suzuki S, Kanai Y, Endou H (2001) Expression of L-type amino acid transporter 1 in a rat model of liver metastasis: positive correlation with tumor size. Cancer Detect Prev 25(5):439–445

Testa B, Kramer SD (2007) The biochemistry of drug metabolism—an introduction—Part 2. Redox reactions and their enzymes. Chem Biodivers 4(3):257–405. doi:10.1002/cbdv.200790032

Verrey F, Closs EI, Wagner CA, Palacin M, Endou H, Kanai Y (2004) CATs and HATs: the SLC7 family of amino acid transporters. Pflug Arch Eur J Phy 447(5):532–542. doi:10.1007/s00424-003-1086-z

Wagner CA, Lang F, Broer S (2001) Function and structure of heterodimeric amino acid transporters. Am J Physiol Cell Ph 281(4):C1077–C1093

Wester HJ, Herz M, Weber W, Heiss P, Senekowitsch-Schmidtke R, Schwaiger M, Stocklin G (1999) Synthesis and radiopharmacology of *O*-(2-[F-18]fluoroethyl)-L-tyrosine for tumor imaging. J Nucl Med 40(1):205–212

Wise DR, Thompson CB (2010) Glutamine addiction: a new therapeutic target in cancer. Trends Biochem Sci 35(8):427–433. doi:10.1016/j.tibs.2010.05.003